IJISET - International Journal of Innovative Science, Engineering & Technology, Vol. 8 Issue 11, November 2021
ISSN (Online) 2348 – 7968 | Impact Factor (2020) – 6.72
www.ijiset.com

Structural and functional elucidation of novel FAB inhibitors: A NMR, Molecular Dynamics, MM/PBSA and Biological Activity Study

Mutyala Veera Venkata Vara Prasad [1,*], Venkata Suryanarayana Ch[2], Vadde Veeranna[3], Radha HR[1] and Sai Subrahmanya Praveen Kumar Darsi [4]

[1] Department of Chemistry, TJohn Institute of Technology, Karnataka Bengaluru, 560076, India

[2] Research & Development, KLIO Pharma Private Limited, Plot No-75,ALEAP Industrial Area, Pragati Nagar, Kukatpally, Hyderabad-500090, Telangana, India

[3]Department of Chemistry, AMC Engineering College, Karnataka, Bengaluru, 560083, India

[4] Department of Chemistry, Jawaharlal Nehru Technological University Hyderabad, Andhra Pradesh, 500085, India

*Corresponding Author E-mail: varamapr9@gmail.com

Abstract

Beta-ketoacyl-acyl carrier protein synthase III (or FABh)is one of the key enzymes for bacterial fatty acid biosynthesis. FABh was extensively studied in *E.coli* by various research groups earlier as a therapeutic target for drug resistant strains. Thus, it became a key target for structure-based drug design to develop novel antibacterial. In our previous study, we screened nearly more than 10 synthesized compounds to test its binding affinity by molecular docking. In the present study, we used top two compounds, A7 and A9, from our previous molecular docking study were subjected to understand their structural and functional features with respect to their binding mode to theFABh enzyme by employing a combination of NMR, molecular dynamics simulations, free energy calculations using the MM/PBSA approach and biological assay activity. Results from MD simulations were extracted to predict the strength of interactions of protein-ligand systems by binding free energy (ΔG_{bind}) calculation obtained from MM/PBSA. The (ΔG_{bind}) was then correlated with experimental IC_{50} values to gain insights into inhibitory activities of two compounds. This study provides structure –function relationship of two novel inhibitors, A7 and A9, with FABh protein.

Keywords: FABh, molecular dynamics, MM/PBSA, NMR, IC_{50}, free binding energy.

Introduction

Beta-ketoacyl carrier protein synthase III or Fatty acid biosynthesis hydrolase (FABh) is a one of the condensing enzymes that is used in fatty acid biosynthesis in bacteria and other higher organisms like plants [1]. The pervasive type III fatty acid system (FAS) in bacteria is not limited to cell viability but there is a significant difference between bacterial fatty acid synthesis and human fatty acid synthesis, inclusive of cellular organization, the structural features of enzymes and their functional roles. Thus, it became a key target for antibacterial chemotherapies [2, 3]. FABh plays a pivotal role in bacterial FAS [4]. It is well understood, FABh, initiates the fatty acid biosynthesis by elongation cycles and its involvement in feedback regulation by product inhibition shows regulatory nature of the enzyme in biosynthesis [5]. Additionally, FABh proteins from both Gram-positive and Gram-negative bacteria shows high sequence and structure conservation, while there is no evidence of homologue proteins to be found in human. The residues lining the active site region of protein seems to be invariant in both the types of bacteria[6]. Surely these key features of this protein favour it to be an attractive target for designing novel antibacterial drugs with high selectivity, low-toxicity and broad-spectrum antibacterial activity [7, 8].

At present, the ascent and predominance of multi-drug resistant virulent bacteria have brought us challenges which escalates the need to create novel antibacterial agents and increase the bio-utility of traditional drugs [9]. Various chemical scaffolds like thiazoles and their congeners have attracted promising interest over the years for their antibacterial activities [10].Improper medications, diets, changing lifestyles and environmental changes has increased the upsurge of thiazoles or analogues drug resistant bacteria.

In perspectives of treating such drug-resistant bacteria, we describe here structural and functional features of synthesized compounds at atomistic level and their biological activity. We first employed NMR study on synthesized compounds and later their biological activity was screened against three Gram-negative bacteria (*E.coli*, *P. aeruginosa* and *K.pneumoniae*) and three Gram-positive bacteria (*S.aureus*, *S.pyogenes* and *B.megaterium*) and fungus(*Cladosporium sp.*) by applying MIT calorimetric method. Further analysis was implemented to gain insights into the mechanism of inhibition by MD simulation in Gromacs and binding free energy (ΔG_{bind}) by MM/PBSA approach. The MD simulation and (ΔG_{bind}) computationswere carried on X-ray crystallographic structure of the FABh of *E.coli*(PDB code: 1HN9)[11]. The (ΔG_{bind}) is correlated with experimental IC_{50} values.

Materials and Methods:

NMR

The synthesized compounds with IUPAC name were given compound id name for better readability in this document. Compound 1-cyclopropyl-6-fluoro-8-methoxy-4-oxo-7-(3-(trifluoromethyl)-5,6-dihydro-[1,2,4]triazolo[4,3-a]pyrazin-7(8H)-yl)-1,4-dihydroquinoline-3-carboxylicacid hydrochloride and 1-cyclopropyl-6-fluoro-7-(4-(6-fluorobenzo[*d*]isoxazol-3-*yl*) piperidin-1-*yl*)-8-methoxy-4-oxo-1,4-dihydroquinoline-3-carboxylic acid hydrochloride is named as A7 and A9 respectively. The method employed for NMR study was as follows:

1-cyclopropyl-6-fluoro-8-methoxy-4-oxo-7-(3-(trifluoromethyl)-5,6-dihydro-[1,2,4]triazolo[4,3-a]pyrazin-7(8H)-yl)-1,4-dihydroquinoline-3-carboxylic acid hydrochloride (A7)

^{1}H NMR (DMSO-d_6, 300 MHz): δ 1.02-1.15(m, cyclopropane ring, 4H), 2.34-2.01(m,2H), 2.18(m, 2H),3.62(m,2H),3.82(s,3H, methoxy),4.20(m, cyclopropane ring,1H), 7.99-7.93(m, J=18Hz,1H,Ar-H), 8.73-8.68(s,1H,olefinic), 14.99(s, 1H, COOH);

1-cyclopropyl-6-fluoro-7-(4-(6-fluorobenzo[d]isoxazol-3-yl) piperidin-1-yl)-8-methoxy-4-oxo-1,4-dihydroquinoline-3-carboxylic acid hydrochloride (A9)

^{1}H NMR (DMSO-d_6, 300 MHz): δ 1.13-1.06(m, cyclopropane ring, 4H), 1.23(m,2H),2.04-2.01(m, *J*=9Hz,2H), 2.18(m, 2H),3.61(m,2H),3.82(s,3H,methoxy)3.43(m,1H),4.20 (m, cyclopropane ring,1H), 7.36-7.33(m, *J*=9Hz,1H,Ar-H),7.80-7.72(m, *J*=24Hz, 2H,ArH), 8.08(m,1H, Ar-H) ,8.72 (s,1H,olefinic proton),14.99(s,1H,COOH);

Molecular dynamics simulation

MD simulation of the protein-ligand system was carried out using the GROMOS96 54a7 force field [12] of the GROMACS 5.0 package [13]. From previous study of molecular docking [ref], the top two compounds namely A7 and A9which showed lowest binding energy (most negative) in the docking experiment were taken as an initial conformation for conducting each MD simulations separately. The topology parameters of proteins were created by default Gromacs program. The parameters to create topologies for both ligands were generated by ATB server[14]. The complex was immersed in a dodecahedron of extended simple point charge water molecules [15]. Energy minimization was performed

using the steepest descent method of 1000 steps followed by the conjugate gradient method for 1000 steps, to remove any bad contacts. Position-restrained dynamics simulation (equilibration phase) (NVT and NPT) of the system was done at 300 K for 1000 ps followed by MD production run for 10 ns each for both the ligands. The long-range electrostatics were computed by Particle-Mesh-Ewald(PME) [16] summation at a cut-off distance 12 Å. A total of 30 ns MD simulation was carried out in this study one for unbounded protein and other two for bounded protein-ligand complexes each of 10 ns. For the purpose of analysis, the MD trajectories were saved at every 1.0 ps throughout the simulation time. All the structural images were generated using Discovery Studio 3.5 Visualizer[17].

MM/PBSA calculation

The Molecular Mechanics/ Poisson-Boltzmann Surface Area (MM/PBSA) method [18] is regarded as one of the most accepted method for calculating binding free energy (ΔG_{bind}). A total number of 100 snapshots from the last 2 ns MD trajectory at an interval 10 ps for binding energy calculation using g_mmpbsa tool [19]. Binding free energy (ΔG_{bind}) can be calculated by the equation:

$$\Delta G_{bind} = G_{complex} - (G_{protein} + G_{ligand}) \quad (1)$$

Where

$G_{complex}$= Total free energy of protein-ligand complex

$G_{protein}$ = Free energy of protein alone in solvent

G_{ligand} = Free energy of ligand alone in solvent

The free energy for individual parameters in above equation is given by:

$$G_a = E_{MM} + G_{solvation} \quad (2)$$

Where a can be protein, ligand or complex

E_{MM}= Average molecular mechanics potential energy in vaccum

$G_{solvation}$ = Free energy of solvation

The molecular mechanics potential energy can be computed by equation:

$$E_{MM} = E_{bonded} + E_{non\text{-}bonded} = E_{bonded} + (E_{vdw} + E_{elec}) \quad (3)$$

Where E_{bonded} is bonded interaction due to bond, angles, dihedrals and improper interactions. $E_{non\text{-}bonded}$ is due van der Walls and electrostatic interactions. Generally, ΔE_{bonded} is treated to be zero [8].

The solvation free energy ($G_{solvation}$) is estimated by equation:

$$G_{solvation} = G_{polar} + G_{non\text{-}polar} \quad (4)$$

Where G_{polar} was calculated using the Poisson-Boltzmann (PB) equation [9] and $G_{non\text{-}polar}$ computed from solvent-accesible surface area (SASA) by the following equation:

$$G_{non\text{-}polar} = \gamma SASA + b \quad (5)$$

Where γ is the surface tension coefficient and b is adjusting parameter. The constant values are:

$\gamma = 0.0054$ Kcal/Mol/Å^2

b = 0.916 Kcal/Mol

RESULTS AND DISCUSSIONS

Antibacterial and antifungal activities

The compounds (A7 and A9) were screened for antibacterial activity against three Gram-positive bacteria: *S.aureus*, *S.pyogenes* and *B.megaterium* and three Gram-negative bacteria: *E.coli*, *P. aeruginosa* and *K.pneumoniae*. Also, we tested on fungus named *Cladosporium sp* for antifungal gactivity by MIT calorimetric method [20]. The inhibitory concentration values of these compounds were illustrated in Table 1.

Compounds / Microorganisms	Gram-positive		Gram-negtive				Fungal
	S.aureus	*S.pyogenes*	*B.megaterium*	*E.coli*	*P. aeruginosa*	*K.pneumoniae*	*Cladosporium sp.*
A7	33.57	**19.33**	**18.57**	**13**	**20**	**15**	**21.33**
A9	43.57	32.33	26.66	29	36	26	29.57
Std	**24.11**	28.66	31.57	21.2	21	22	40

Table 1. Inhibitory concentration values (µg/ml) of the synthesized compounds and control(Std). Best IC50 values highlighted in bold.

Standard antibacterial agents were taken as positive controls to estimate the potency of synthesized compounds under similar conditions. The results showed that compound A7 showed better IC50 values against *S.pyogenes* and *B.megaterium* in Gram-positive class

group than standard ones. Similarly, it can be seen that compound A7 is almost best against *E.coli* followed by *K.pneumoniae* in Gram-negative class group on scale of IC_{50} values. It is quite evident from above table that the synthesized compound A7 has better anti-bacterial activity even with standard antibacterial agents though it has also good anti-fungal activity too. The plausible reason for such activity at atomic scale was further analysed from MD simulation and free binding energy (ΔG_{bind}).

MD Simulation analysis

In the present study, MD simulations for FABh-inhibitor complexes, A7 and A9, (shown in Fig 1) were conducted for 10 ns each.

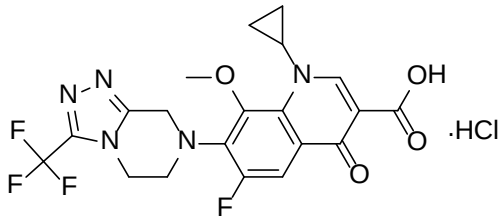

1-cyclopropyl-6-fluoro-8-methoxy-4-oxo-7-(3-(trifluoromethyl)-5,6-dihydro-[1,2,4]triazolo[4,3-a]pyrazin-7(8H)-yl)-1,4-dihydroquinoline-3-carboxylic acid hydrochloride

A7(1a)

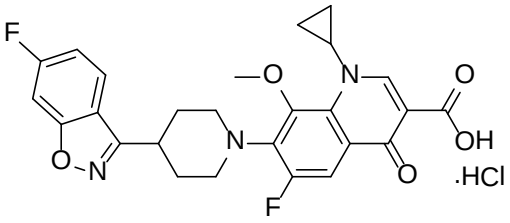

1-cyclopropyl-6-fluoro-7-(4-(6-fluorobenzo[d]isoxazol-3-yl) piperidin-1-yl)-8-methoxy-4-oxo\-1,4-dihydroquinoline-3-carboxylic acid hydrochloride

A9(1b)

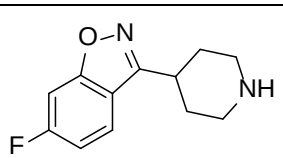

1a

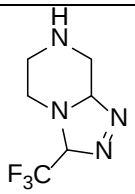

1b

Fig 1. The chemical structures of two compounds (1a) A9and (1b) A7

The reliability of MD simulation of protein-ligand complexes is estimated by the Root-Mean-Square Deviation (RMSD) of the backbone atoms relative to the starting minimized structures of the complexes as a function of time. RMSD of two complexes and protein (shown in Fig 2) establishes the stability of complexes throughout the phase of simulation. It can be seen from the RMSD plot FABh-A7 complex converged after 5ns and then reached equilibrium at an average RMSD of 0.24nm. Also, the complex shows close agreement with RMSD of protein alone throughout the MD trajectories. FABh-A9 complex showed equilibrium after 7ns of the simulation time with an average RMSD of 0.28nm. These results showed that trajectories of MD for both complexes are stable at 8ns to 10ns simulation time.

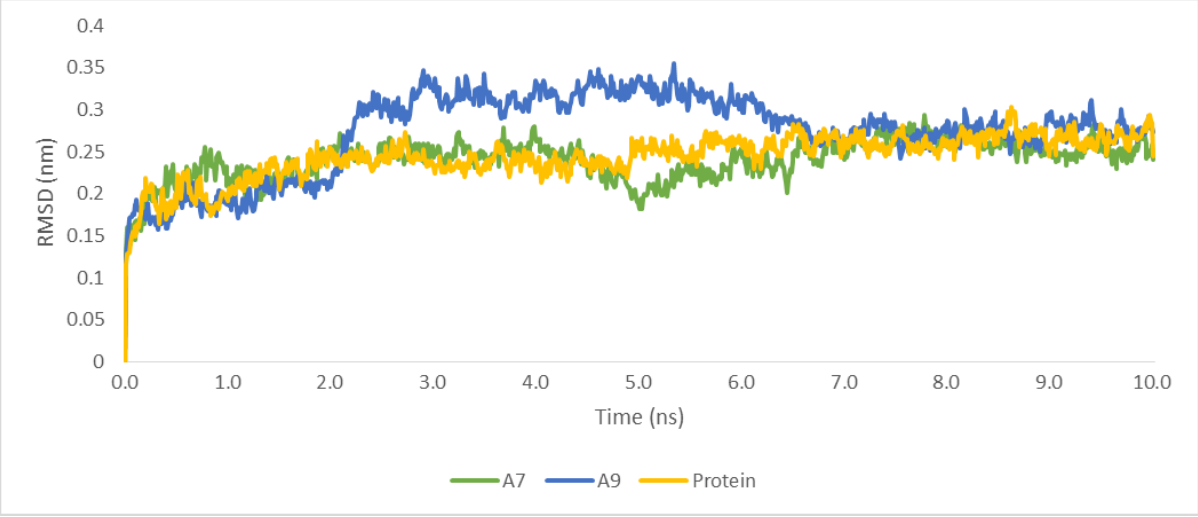

Fig 2. The root-mean-square deviations (RMSD): A7 (green), A9 (blue) and protein (yellow)

Further detailed analysis of Root-Mean-Square Fluctuation (RMSF) versus the protein residue numbers for FABh-A7 complex and FABh-A9 complex is illustrated in Fig 3. In this figure it is clearly shown that both protein-inhibitor complexes show similar rmsf distributions with FABh protein. The active site residues, Cys112, His244, Asn274 etc. show a stiff behaviour for both the complexes.

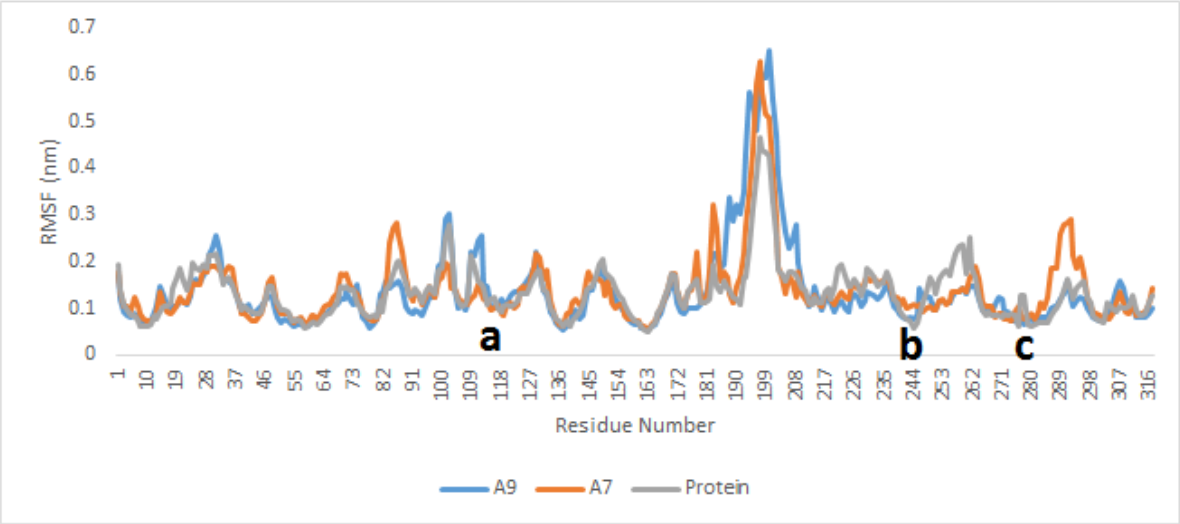

Fig 3.RMSF of backbone atoms (CA, N, C) versus residue numbers of both the complexes and protein: A9 (blue), A7 (red) and protein (gray). The residues a, b and c were Cys112, His244 and Asn274 respectively.

The MD structures were extracted from snapshots of 8 ns to 10 ns where the complexes showed stability and superimposed to each other for visual analysis (shown in Fig 4.)

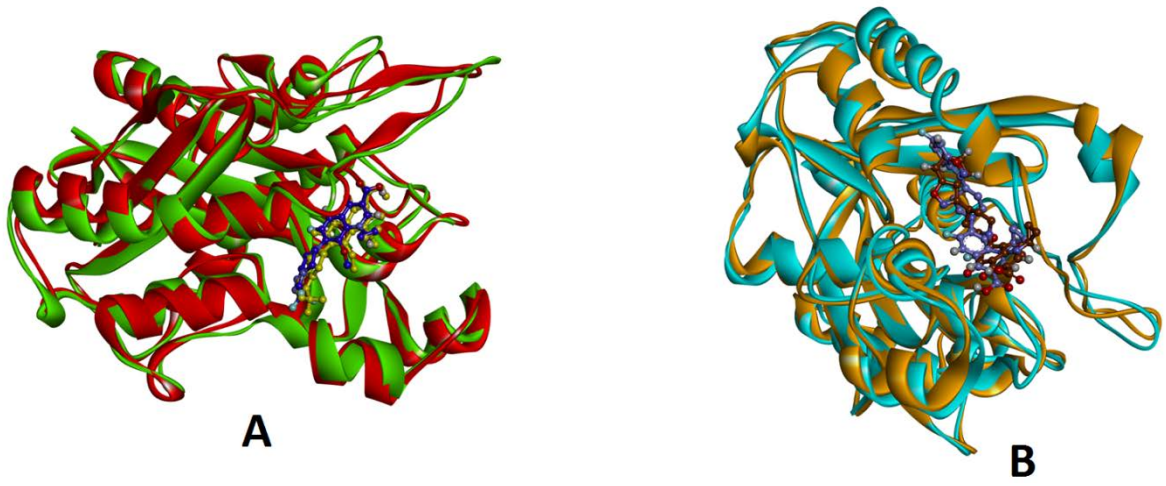

Fig 4. The superimposed structures of FABh-inhibitor complexes (A)FABh-A7 complex (red at 8ns and green at 10ns) and (B) FABh-A9 complex (yellow at 8ns and sky blue at 10 ns). The cartoon representation shown for protein and ball-stick shown for ligands.

By visual analysis, it is clear that there was a less motional deviation in backbone atoms of protein when bound with respective ligands as the secondary structures of protein were remain intact with ligands at time interval of 8 ns to 10 ns of simulation time. There is a subtle fluctuation in loop regions.

Calculation of Binding Free Energies by MM/PBSA

The MM/PBSA method was employed to calculate the binding free energies (ΔG_{bind}) by implementing single trajectory protocol. The 100 snapshots were retrieved at a time interval of 10 ps from the last 2 ns of MD trajectories for the analysis of binding free energy. The computed binding free energies and parameters are listed in Table 2.

Compounds	Van der waal (kJ/mol)	Electrostatic (kJ/mol)	Polar solvation (kJ/mol)	Non-polar solvation(kJ/mol)	Binding energy(ΔGbind) (kJ/mol)
A7	-17.121±51.787	-0.479±4.159	7.072±28.552	-2.301±6.045	-12.830±42.031
A9	0.00±0.00	-0.221±0.134	-6.999±6.318	-0.324±0.683	-7.543±6.325

As shown in Table 2, compound A7 showed best free binding energy (ΔG_{bind}), (-12.8kJ/mol) than A9 (-7.54 kJ/mol) when forms complex with FABh protein. Both intermolecular van der waal and non-polar solvation interactions play the most important contributions in binding in case of FABh-A7 complex while there is no interaction due to polar solvation energy in the active site region of the complex.

Residue wise free energy decomposition

Residue wise decomposition free energy was also calculated from MM/PBSA to understand which key residues are important to help in binding of ligands within the active site region of the desired protein, here FABh. The illustration of per residue decomposition energy is shown in Fig 5.

A

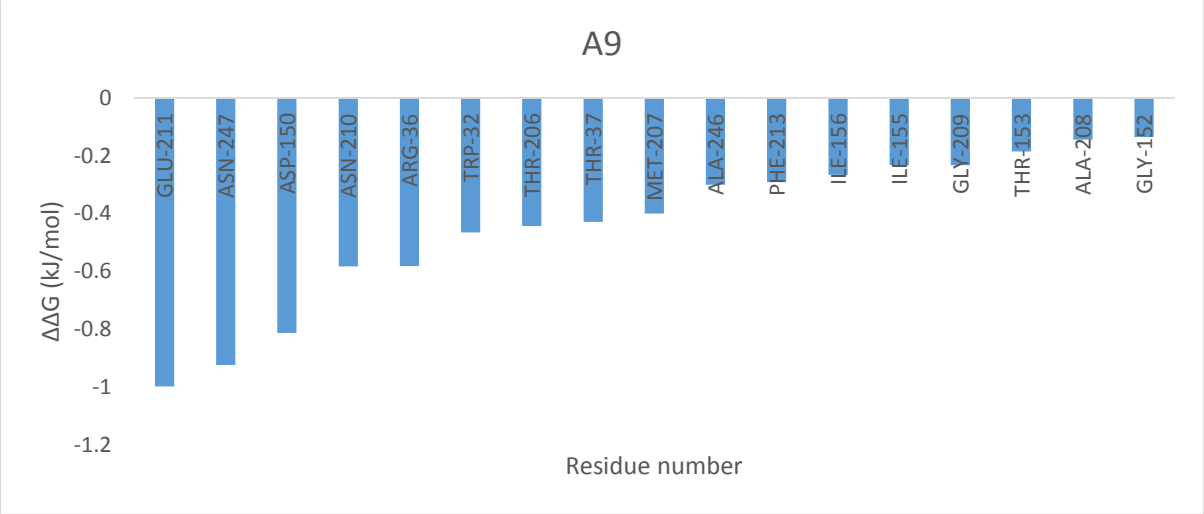

B

Fig5. Per residue energy decomposition of (A) A7 and (B) A9 FABh complexes

As shown in above figure, the residue wise free energy calculations (ΔΔG) for both the complexes were carried out by extracting active site region around 5 Å of respective ligands. Although it is clear from figure that the residues involved in binding of FABh-A9 complex does not contribute to any non-favourable interactions (all negatives) but overall free binding energy(ΔG_{bind}) is lesser than FABh-A7 complex from table 2. Also, it is evident from Fig 5A that the residues which shows unfavourable interactions (ASP27 and ASN210) may contributed in polar solvation energy from table 2 as positive values. Overall, the MM/PBSA results is better for compound A7 than A9.

The key interactions of A7 and A9 complexes with residues are visualized and analysed as shown in Fig6.

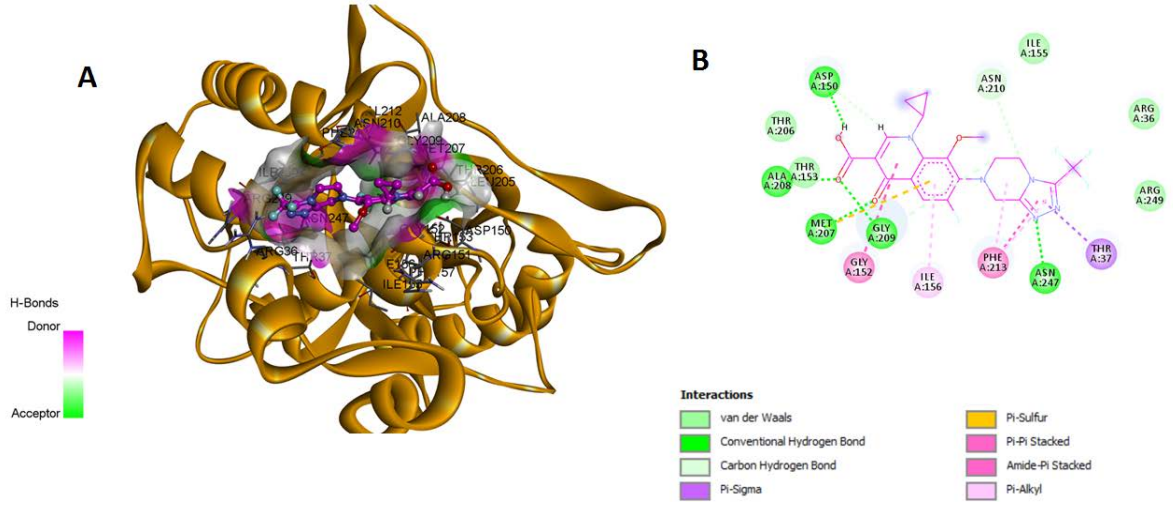

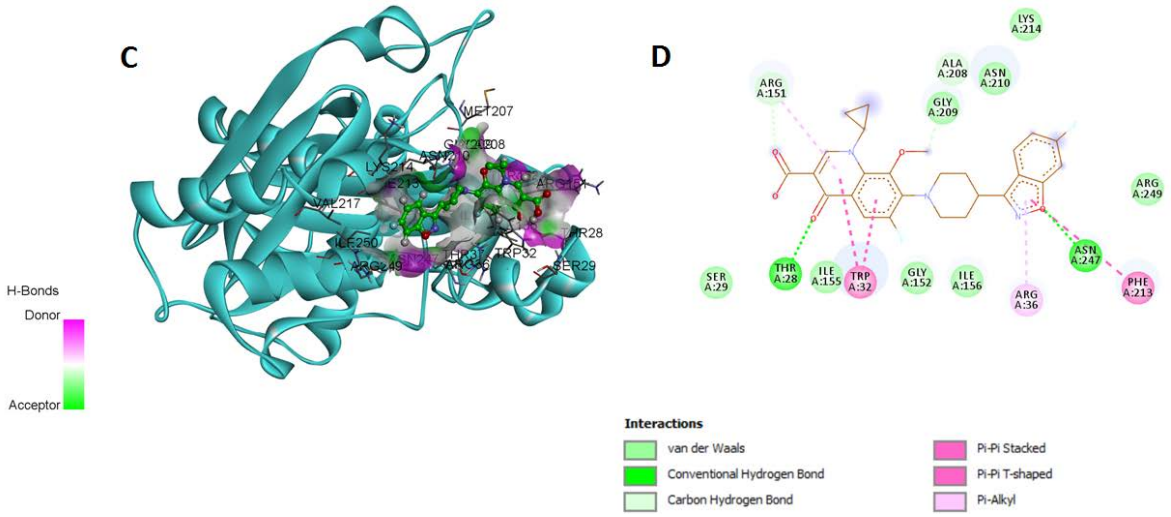

Fig 6. Binding mode of FABh-inhibitors complex with key residues (A) FABh-A7 complex: Protein(yellow cartoon), residues(sticks) and ligand(pink ball-stick) (B) 2D representation of binding modes and (C)FABh-A9 complex: Protein (sky blue cartoon), residues (sticks) and ligand (green ball-stick) (D) 2D representation of binding modes

Conclusion

A combined approach of a NMR, biological activities, MD simulation and MM/PBSA calculations resulted in identifying novel antibacterial agent against FABh protein. The experimental inhibitory assay is truly validated by free binding energy (ΔG_{bind}) obtained from MM/PBSA calculations. In biological activity experiment, compound A7 has broader activity against various bacterial strains than A9 and standard ones. From MD simulations and MM/PBSA, A7 showed better results in RMSD, RMSF and structural superimposition. The (ΔG_{bind}) for A7 is ~ -13 kJ/mol which is in close agreement with IC_{50} values for some Gram-negative bacteria in range of 13-15(µg/ml) and 17-19(µg/ml) for Gram-positive ones. Based on residue wise free energy decomposition and structural analysis, the difference of binding free energy for compound A7 is estimated by Arg36, Ile155, Gly152, Ala208, Gly209, Asn247 and Arg249. In addition to it, the presence three fluoro groups at methyl position in A7 structure favour more hydrogen bonds and vander waal interactions. The results predicted from this study will be beneficial for rational design of novel antibacterial agents in future.

References

1. Lai, Chiou-Yan, and John E. Cronan. "β-Ketoacyl-acyl carrier protein synthase III (FABh) is essential for bacterial fatty acid synthesis." *Journal of Biological Chemistry*. **2003**, 51494-51503.

2. Khandekar, Sanjay S., *et al*., "Identification, Substrate Specificity, and Inhibition of theStreptococcus pneumoniae β-Ketoacyl-Acyl Carrier Protein Synthase III (FABh)." *Journal of Biological Chemistry* **2001**, 30024-30030.
3. Qiu, Xiayang, et al. "Refined structures of *β*-ketoacyl-acyl carrier protein synthase III." *Journal of molecular biology* , **2001**,307.1 , 341-356.
4. Khandekar, Sanjay S., Robert A. Daines, and John T. Lonsdale. "Bacterial *β*-ketoacyl-acyl carrier protein synthases as targets for antibacterial agents." *Current Protein and Peptide Science* . **2003**,4.1, 21-29.
5. Heath, Richard J., and Charles O. Rock. "Inhibition of-ketoacyl-acyl carrier protein synthase III (FABh) by acyl-acyl carrier protein in Escherichia coli." *Journal of Biological Chemistry.* **1996**.271.18 , 10996-11000.
6. Nie, Zhe, *et al.* "Structure-based design, synthesis, and study of potent inhibitors of β-ketoacyl-acyl carrier protein synthase III as potential antimicrobial agents." *Journal of medicinal chemistry.* **2005**.48,5 , 1596-1609.
7. Wang, Jun, *et al.* "Discovery of platencin, a dual FABf and FABh inhibitor with in vivo antibiotic properties." *Proceedings of the National Academy of Sciences.* **2007**,104.18 (2007): 7612-7616.
8. Heath, Richard J., and Charles O. Rock. "Fatty acid biosynthesis as a target for novel antibacterials." *Current opinion in investigational drugs* (London, England: 2000) , **2004**, 5,2, 146.
9. Leeb, Martin. "Antibiotics: a shot in the arm." *Nature*, 2004,4,31,892-893.
10. Kitagawa, Hideo, *et al.* "Phenylimidazole derivatives of 4-pyridone as dual inhibitors of bacterial enoyl-acyl carrier protein reductases FabI and FabK." *Journal of medicinal chemistry*. **2007**, 50.19 , 4710-4720.
11. Qiu, Xiayang, *et al*. "Crystal Structure of β-Ketoacyl-Acyl Carrier Protein Synthase III A KEY CONDENSING ENZYME IN BACTERIAL FATTY ACID BIOSYNTHESIS." *Journal of Biological Chemistry* . **1999**, 274,51, 36465-36471.
12. Schmid, Nathan, *et al*. "Definition and testing of the GROMOS force-field versions 54A7 and 54B7." ., **2011**. 40,7 , 843.
13. Van Der Spoel, David, *et al*. "GROMACS: fast, flexible, and free." *Journal of computational chemistry*. **2005**. 26,16, 1701-1718.
14. Malde, Alpeshkumar K., *et al.* "An automated force field topology builder (ATB) and repository: version 1.0." *Journal of chemical theory and computation*. **2011**, 7.12, 4026-4037.

15. Zielkiewicz, Jan. "Structural properties of water: Comparison of the SPC, SPCE, TIP4P, and TIP5P models of water." *The Journal of chemical physics*, **2005**, 123,10 , 104501.
16. Darden, Tom, Darrin York, and Lee Pedersen. "Particle mesh Ewald: An N· log (N) method for Ewald sums in large systems." *The Journal of chemical physics*, **1993**, 98,12, 10089-10092.
17. Discovery Studio 3.5 (Accelrys Software, Inc., San Diego, CA)
18. Massova, Irina, and Peter A. Kollman. "Combined molecular mechanical and continuum solvent approach (MM-PBSA/GBSA) to predict ligand binding." *Perspectives in drug discovery and design*, **2000**, 18,1, 113-135.
19. Kumari, Rashmi, Rajendra Kumar, and Andrew Lynn. "g_mmpbsa. A GROMACS Tool for High-Throughput MM-PBSA Calculations." *Journal of chemical information and modelling*, **2014**, 54, 7 ,1951-1962.
20. Shi, Lei, *et al.*, "Design and synthesis of potent inhibitors of β-ketoacyl-acyl carrier protein synthase III (FABh) as potential antibacterial agents." *European journal of medicinal chemistry*, **2010,** 45,9 , 4358-4364.